Enhancing Synchronization in Systems of Non-identical Kuramoto Oscillators

Markus Brede

CSIRO Marine and Atmospheric Research, Canberra ACT 2602, Australia
Markus.Brede@Csiro.au

Abstract. In this paper we present a summary of some of our recent results on the synchronization of non-identical Kuramoto oscillators coupled via complex networks. Crucially, we emphasize that the systems overall degree of synchronization cannot only be improved by tuning properties of the coupling network, but also by a correlated assignment of oscillators to nodes. In the context of symmetrical coupling via undirected networks we discuss network characteristics and correlations between the oscillator placement on the nodes of the network that enhance the overall degree of synchronization. Several simple rules to improve the degree of synchronization in a system are given, such as, e.g. (i) anti-correlated placement of adjacent oscillators, and (ii) placement of oscillators with native frequencies far off the mean in the centre of the network and (iii) placement of oscillators with native frequencies close to the mean at the periphery of the network. The influence of oscillator correlations on synchronization transition is discussed as well. Finally, we analyze the question whether a a globally synchronized system can be generated by rewirings that improve the local synchronizability.

Keywords: Synchronization, non-identical oscillators, Kuramoto, networks.

1 Introduction

Synchronization problems are pertinent to a plethora of distributed biological and man-made systems. Examples are found among pacemaker cells, many other types of cells, fireflies that flash in unison and more biological systems, see, e.g. [1,2], social phenomena as oppinion formation [4], but also in physical engineered systems, such as arrays of Josephson junctions [3] or power systems [5], see also [6] for a recent review. The importance of the problem has attracted much attention in the literature in recent times. Notably, since it was understood that the coupling between the elements in most of these distributed systems occurs via complex networks [7,8], understanding the collective dynamics of synchronization on complex networks has become a major focus of research. So far, much attention has been paid to network properties that facilitate synchronization between identical oscillators. Most work on this problem focuses on an investigation of the fully synchronized state via the Master stability function approach

J. Zhou (Ed.): Complex 2009, Part II, LNICST 5, pp. 1955–1966, 2009.

pioneered by Pecora and Carroll [9]. Results about structural features of networks that give rise to more stable synchronized states are manifold. Findings include, that degree-homogeneity, low degree of clustering, short pathlengths, load-balancing on links and nodes and disassortative degree-mixing facilitate synchronization [10,11].

However, as in most natural or man-made systems, oscillators differ slightly from each other, the problem of the synchronization of non-identical oscillators appears the more relevent issue. In this context, the emphasis of research naturally shifts from being purely focused on properties of the coupling network to also take account of correlations between oscillator identity and properties of the node an oscillator is placed at. The problem of optimizing a networked system of non-identical oscillators thus becomes one of studying the co-evolution of network properties and oscillator correlations.

In the following, as a proto-typical example for phase synchronization, we study the model system introduced by Kuramoto [2]

$$\dot{\phi}_i = \omega_i + \sigma \sum_{j=1}^{N} a_{ij} \sin(\phi_j - \phi_i), \tag{1}$$

where the ϕ_i denote the phases of N limit-cycle oscillators, the ω_i their native frequencies and the matrix $A = (a_{ij})$ the coupling network, while σ is the coupling strength. The coupling matrix A is given by the adjacency matrix of the coupling network, i.e. $a_{ij} = 1$ if there is a link from i to j and $a_{ij} = 0$ otherwise. The model (1) has been widely studied, both analytically and numerically (see [12] for a recent summary). It arises in the weak-coupling limit of coupled limit-cycle oscillators.

The degree of synchronization of the system (1) is conveniently measured by introducing the quantities r and Φ via

$$r(t) \exp(i\Phi(t)) = \sum_j \exp(i\phi_j(t)), \tag{2}$$

where $r(t)$ denotes the amplitute and $\Phi(t)$ the average phase of all the oscillators. For desynchronized oscillators one has $r(t) \propto 1/\sqrt{N}$, whereas $r(t) = \mathcal{O}(1)$ if (partial) macroscopic synchronization exists. For a given set of initial conditions $\phi_i(t = 0)$ it is often useful to define a time-averaged order parameter $\overline{r} = 1/T \int_{T_{rel}}^{T+T_{rel}} r(t)dt$, which excludes the initial transitient of the dynamics of (1), given by the relaxation time T_{rel}.

The paper will be organized as follows. In section 2 we will discuss the case of the optimized arrangement of systems of symmetrically coupled non-identical Kuramoto oscillators. We first briefly introduce a numerical optimization technique and then discuss the resulting optimized systems. A major finding is that the optimal arrangements are characterized by strong correlations between characteristics of adjacent oscillators. This naturally raises the question about the synchronization transition in correlated oscillator ensembles. Oscillator correlations are a concept that enherently pertains to sparsely coupled systems. We

will demonstrate that, indeed, oscillator correlations can systematically shift the critical point and even the critical exponents.

A further question that naturally appears in the context of synchrony-optimized networks is whether global synchronization can be achieved in systems with only local information, which will be investigated next. A brief discussion of the problem concludes the second section.

Finally, in the last section we summarize the above results and hypothesize about some general principles that facilitate synchronization in networks of non-identical oscillators. Some ideas for future work are presented as well.

2 Symmetrical Coupling – Undirected Networks

2.1 Optimal Configurations

In this section we focus on symmetrical coupling $a_{ij} = a_{ji}$ or undirected networks. The results we present in the following are mainly based on [13,15,16]. Given a number of links $L = 1/2 \sum_{i,j=1}^{N} a_{ij}$, a coupling strength σ^* and a set of native frequencies (that were randomly selected from a uniform distribution over the interval $[-1, 1]$), we ask the question: What is the arrangement of coupling network a_{ij} and oscillator assignment that gives rise to the largest degree of synchronization, i.e. the largest time averaged order parameter $\overline{r}$?

We approach the problem with a numerical optimization scheme. Starting with an adjacency matrix (a_{ij}) that corresponds to an Erdös-Rényi random graph network, the system of equations (1) is integrated for homogeneous initial conditions, e.g. $\phi_i(t = 0) = 0$. This allows the calculation of an average degree of synchronization for the given network and native frequency configuration. Then, iteratively, rewirings in the network (that leave the number of links constant) or changes in the native frequency assignment to nodes are suggested. If an alteration improves the average degree of synchronization $\overline{r}$, it is accepted. Otherwise, the system is restored to its previous state and another random configuration change is suggested. The scheme is repeated until $I = L$ alteration attempts have not lead to an increase in average synchronizability, i.e. until every link has on average been attempted to rewire once.

At first thought, it appears that the results of the above scheme might depend on the specific choice of initial conditions $\phi_i(t = 0) = 0$. However, it turns out that an increase in synchronizability for homogeneous initial conditions also improves the system's average synchronizability for random initial conditions, for which all the $\phi_i(t = 0)$ are independently selected at random from $(-\pi, \pi]$. The reason for this appears to be that the main pressure towards desynchronization stems from the variance in the native frequencies, whereas the heterogeneity in the initial conditions plays only a minor role, mainly influencing the transients [18].

For a small system figure 1a visualizes a typical result obtained from the introduced optimization scheme. While Fig. 1b demonstrates that the optimized network is indeed more synchronizable not only for the specific initial conditions $\phi_i(t = 0) = 0$ but also for averages over randomly chosen initial conditions,

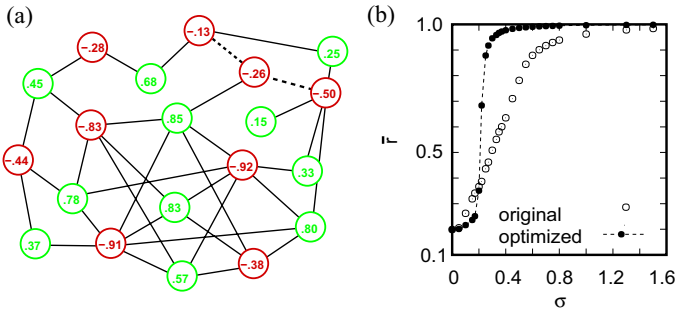

Fig. 1. Example of an evolved optimal configuration for $N = 20$ nodes and $\sigma^* = .3$. (a) the optimized system, red nodes denote negative native frequencies, green nodes positive native frequencies. (b) Dependence of the order parameter on the coupling strength for the system shown on (a). The data points have been obtained as averages over many randomly chosen initial conditions. The data are compared to the dependence of $\overline{r}$ on σ for the random network with which the algorithm was seeded. Figures from [13].

the graphical representation of the network in Fig. 1a clearly shows first indicative correlations between oscillator identity and network structure. Most prominently, one observes that apart from two exceptions (dashed lines in Fig. 1a) oscillators with negative native frequencies are neighbours of oscillators with positive native frequencies. Thus, clearly the native frequencies of adjacent oscillators are strongly anti-correlated, maximizing the time-averaged magnitude of the aggregate interaction term $J = \sum_{i,j} |a_{ij}\overline{\sin(\phi_j - \phi_i)}|$. In fact, this very argument that optimal synchronization in systems of non-identical oscillators will be achieved when average interactions are maximized, suggests that the above finding is not restricted to the Kuramoto system. Investigating whether general anti-correlations between the characteristics of more general (chaotic) oscillators enhances synchronization appears an interesting subject for further research.

Further, in contrast to what has been found for networks of identical oscillators [10], the optimal network is clearly not regular, i.e. not an entangled network in the sense of [10]. Rather, as one would expect for heterogeneous systems, oscillators find a place in the optimal configuration that depends on their native frequency. Accordingly, closer inspection reveals that oscillators with large magnitude of their native frequency tend to be associated with nodes of relatively large degree, while oscillators with native frequencies close to the the mean (and thus synchronization-) frequency $\langle\omega\rangle = 0$ are associated with nodes of relatively low degree. Such an arrangement appears reasonable from two points of view.

First, one would naturally expect that oscillators with native frequencies deviating strongly from the synchronization frequency $\omega = 0$ would require more input to be drawn towards the collective dynamics. This is equivalent to a requirement for having a larger degree. Second, placing far-off the mean oscillators on hub nodes allows for a more anti-correlated oscillator arrangement, i.e. stronger average interactions.

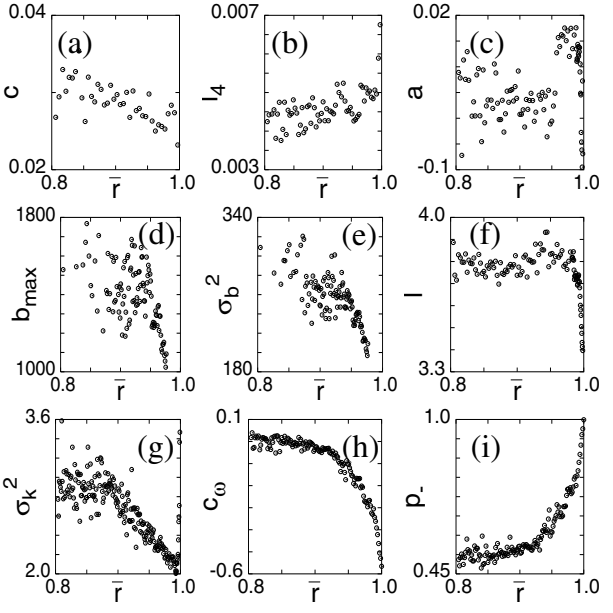

Fig. 2. Dependence of the clustering coefficient (a), density of 4-loops (b), assortativeness (c), maximum load (d), load variance (e), average pathlength (f), degree variation (g), fraction of plus-minus pairs (h) and of the correlation of adjacent native frequencies (i) on synchronizablity measured by $r(\sigma^*)$ during the optimization. The data are for a network of 100 nodes with connectivity $\langle k \rangle = 3.5$. The initial network corresponded to an ER r.g., for other initial conditions like scale-free networks or regular random graphs similar trends are found. Figure from [13].

The data displayed in Fig. 2 give a more systematic investigation of changes in the system's properties as it is evolves towards a more synchronizable state. Panels (a)-(i) monitor the evolution of various network properties as a network is gradually evolved from a random inital frequency assignment and connection pattern towards a synchrony-optimizing configuration. Notably, we observe that while the clustering coefficient is decreasing, the density of 4-loops increases, the network gradually becomes disassortative, maximum load and load variance decline and average pathlengths become smaller. On the same token, the degree variance decreases. All these observations are in agreement with what has been discussed in the literature before in the context of synchronization of identical oscillators [10]. However, changes in network properties are relatively minor in comparison to changes in the arrangement of oscillators. To quantify the latter, we measure the fraction p_- of adjacent oscillators with negative frequencies of opposite signs amongst all pairs of adjacent oscillators and a standard correlation coefficient

$$c_\omega = \frac{\sum_{i,j} a_{ij}(\omega_i - \langle\omega\rangle)(\omega_j - \langle\omega\rangle)}{\sum_{i,j} a_{ij}(\omega_i - \langle\omega\rangle)^2}, \tag{3}$$

between the native frequencies of adjacent oscillators. The evolution of both quantities as the degree of synchronization increases is given in panels (h) and (i). In the optimal configuration virtually all oscillators end up being paired with oscillators with native frequencies of opposite sign.

While confirming that network properties that facilitate synchronization in systems of identical oscillators are also associated with improved synchronization in systems of non-identical oscillators, we thus demonstrate that the actual oscillator arrangement on the coupling network strongly influences synchronization properties as well. It appears worthwhile to stress, that such correlated oscillator arrangements are only possible on sparsely coupled systems. The denser the coupling network, the more 'frustration' is introduced and the less correlated can the oscillator arrangement be (Trivially, in a fully connected system no oscillator correlations can be introduced).

2.2 The Synchronization Transition in Correlated Oscillator Ensembles

Our above experiment strongly suggests that oscillator correlations have an important impact on the synchronization transition of Kuramoto oscillators on networks. The synchronization transition of non-identical Kuramoto oscillators on complex networks has found much attention in the recent literature, see, e.g. [15,16,17,19,20,21,22]. In contrast to the transition for identical oscillator systems which is discontinuous, this is a second order transition. Various studies discuss the role of the network structure on the transition, i.e. the critical point and the universality class of the transition, given by the critical exponents. Close to the critical point the order parameter $\overline{r}$ is found to obey the finite size scaling relation

$$\overline{r}(N,\sigma) = N^{-\alpha} F((\sigma - \sigma_c) N^{1/\nu}), \tag{4}$$

where the function $F(x)$ is a universal scaling function that is bounded in the limit $x \to \pm\infty$, ν is the finite size scaling exponent and α is a critical exponent that is related to the exponent β that describes the dependence of the order parameter on the control parameter in the thermodynamic limit via $\alpha = \beta/\nu$.

To systematically explore the role of oscillator correlations on the synchronization transition on complex networks we proceed as follows. We construct a given coupling network as an Erdös-Rényi random graph with given number of links and select a desired degree of oscillator correlations c^*_ω, cf. Eq. (3). We chose Erdös-Rényi-type random graphs, because for this choice of coupling network the synchronization transition is of the same type as for the all-to-all coupled system, for which it has been well-explored. In this reference case one has $\beta = 1/2$ and $\nu = 2$, which also holds for small-world networks [19]. Deviations from the known behaviour can thus be attributed to the effect of correlated oscillator arrangements.

To proceed, the native frequencies of oscillators are randomly selected from $[-1, 1]$. Next, swaps between the native frequencies of randomly selected oscillator pairs are suggested and accepted, if they lead to a reduction in the difference

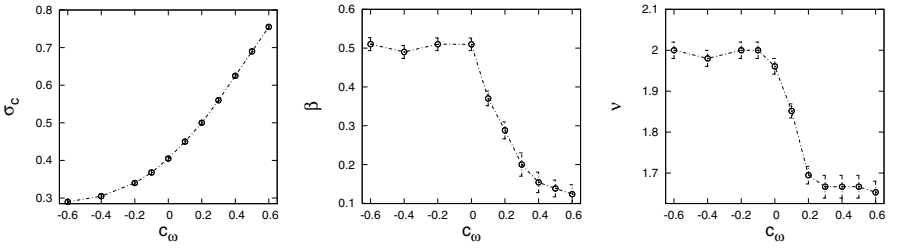

Fig. 3. Dependence of (a) the critical point, (b) the critical exponent β, and (c) the critical exponent ν on the strength of oscillator correlations. Results are obtained from a finite size scaling analysis, cf. text. Figure from [16].

between the actual and the desired level of correlation $|c_\omega - c^*_\omega|$. The procedure is terminated when $|c_\omega - c^*_\omega| < \epsilon$, where we select $\epsilon = 10^{-4}$ for the rest of the study. Clearly, the possible maximum/minimum strength of oscillator correlations depends on the type of coupling network and its link density. For the purpose of this study and a choice of average degrees $\langle k \rangle = 3.5$ (for which we have verified that the networks are connected), oscillator correlations in the range $c_\omega = -.6, ..., .6$ can easily be generated.

Next, equation (4) can be used as the basis of a finite size scaling analysis, with which the critical exponents and the critical coupling can be determined. Plotting, e.g., rN^α vs. the coupling strength σ, one realizes from (4) that curves for different system sizes intersect at a unique crossing point σ_c. Thus, systematically varying α till the $N^\alpha r(N, \sigma)$-curves intersect at one unique point allows to determine the critical exponent α and the critical point σ_c. One further observes from (4) that plots of $N^\alpha r$ vs. $(\sigma - \sigma_c)N^{1/\nu}$ should be independent of the system size N close to the critical point. Thus, having already determined α and σ_c the exponent $1/\nu$ can be found as the value that allows for the best data collapse. The results of the finite size scaling analysis that we present below are based on system sizes ranging from $N = 200$ up to $N = 6400$ oscillators.

The panels in Fig. 3 summarize the results from the finite size scaling analysis. First, in agreement with the observations of the previous subsection, one notes that decreasing correlations between adjacent oscillator pairs induces a transition towards synchronization for lower coupling strengths, whereas introducing strong positive oscillator correlations increases the critical coupling strength. This strengthens the main contention of subsection 2.1 and demonstrates that the results obtained from the optimization of small systems are not finite size effects, but also hold in the thermodynamic limit.

Another important observation from Fig. 3 is that positively and negatively correlated oscillator arrangements appear to represent fundamentally different regimes. Whereas (within reasonable error bounds) the exponents β and ν are unchanged and the same as for the all-to-all coupled system for all neutrally and negatively correlated arrangements, i.e. for $c_\omega \leq 0$, introducing positive correlations between the native frequencies of adjacent oscillators leads to a systematic shift of the universality class of the transition with the correlation

strengths. For $c_\omega > 0$, increasing the correlation strength systematically reduces the exponents β and γ.

The latter observations appears particularly interesting, as changes of critical exponents have so far only been reported when the coupling network is changed. Our findings here demonstrate that correlations within oscillator arrangements can have an equally important effect on the synchronization transition as the topology of the coupling network. Thus measuring the characteristics of the synchronization transition in a black-box system of non-identical oscillators one could not draw inferences about, e.g., the heterogeneity of the topology of the coupling network from the critical exponents. For a more elaborate description and more details of the analysis we refer the reader to Ref. [16].

2.3 Local vs. Global Synchronization

In the above procedure of subsection 2.1 the optimization is performed by evaluating the amplitude order paramater r, i.e. a quantity that measures the 'global' degree of synchronization between all pairs of oscillators in the system at each iteration. Thus, to decide whether a reconfiguration is accepted, global information about all oscillators in the system is required. One may ask the question whether a system where reconfigurations can only be based on local information (or a combination of local and global information) can reach the same synchrony-optimized structure that we discussed before. Such a question appears particularly relevant for biological systems whose fitness depends on the synchronized action of all its constituents. This issue is analyzed in more detail in [15] and we summarize some key results briefly below.

Local synchronization between oscillators can be measured by the order parameter r_{link} introduced by [23,24]:

$$r_{\mathrm{link}} = 1/L \sum_{(k,l)} \left| \lim_{\Delta T \to \infty} 1/\Delta T \int_{T_{\mathrm{rel}}}^{T_{\mathrm{rel}}+\Delta T} e^{i(\phi_l(t)-\phi_k(t))} dt \right|, \tag{5}$$

where T_{rlink} is the relaxtion time, L the number of links and the summations extends over all connected pairs of oscillators. Thus, Eq. (5) effectively averages over the degree of synchronization between between all pairs of connected oscillators.

For the following, it is essential to understand the difference between the order parameters r, cf. Eq. (2), and r_{link}. Clearly, if $r \approx 1$ then also $r_{\mathrm{link}} \approx 1$, i.e. a globally synchronized system is also locally synchronized. However, it is possible to have $r_{\mathrm{link}} \approx 1$ whithout global synchronization, i.e. $r \ll 1$. An example where the latter situation can occur are strongly modular networks. In such systems, for a coupling strength σ that allows for synchronization within the cliques, but yet no global synchronization, most connected pairs of oscillators are situated within cliques. Thus, since they are synchronized with each other, they contribute to r_{link}. Only the relatively few links that connect different modules do not contribute to r_{link}. They, however, constitute only a small fraction of all the links in the network and thus $r_{\mathrm{link}} \sim \frac{\text{links within cliques}}{L} \sim 1$. However,

since the individual cliques are generally not synchronized with each other $r \sim 1/\sqrt{\text{number of cliques}}$.

According to [15] for a given coupling strength σ^* a combined measure of local and global synchronization can be introduced via

$$R(\lambda) = \lambda r + (1 - \lambda) r_{\text{link}}. \tag{6}$$

The parameter lambda interpolates between a situation where the systems' fitness is exclusively defined by global synchronization ($\lambda = 1$) and a situation where the local synchronization measure dominates ($\lambda = 0$). The latter situation can be interpreted as a scenario where agents have only local information, i.e. only information about how well they are synchronized with their network neighbours, to optimize their position in the network.

To explore the trade-off between local and global information we employ a similar numerical optimization procedure as introduced in subsection 2.1. Starting from a random Erdös-Rényi network with randomly assigned frequencies (that were again randomly chosen from the uniform distribution over $[-1, 1]$) the dynamical system given by Eq.'s (1) is integrated numerically for $\phi_i(t = 0) = 0$, which allows the calculation of the order parameters r and r_{link}. Then link rewirings are suggested and the acceptance of such suggestions is based on the fitness measure defined by Eq. (6).

In the limiting case $\lambda = 1$ the results of subsection 2.1 are reproduced, while for $\lambda = 0$ no large degree of global synchronization can be achieved. Rather, even in a highly synchronized initial network configuration, cliques of oscillators with similar native frequencies are formed. The coupling network evolves towards a configuration that maximizes the connectedness within cliques, while minimizing the impact of seperate cliques on each other. The resultant network structure is thus one with high concentrations of intra-clique links and a very small number of inter-clique links, which are mainly an artifact of having enforced the connectedness of the system.

In the case of intermediate values of λ the set of different optimal network configurations becomes much richer. It turns out that the general structure of systems optimizing (6) is independant of the choice of $0 < \lambda < 1$, but is mainly determined by the total amount of available coupling $C = \sigma^* L$ in the system. If C is small, improvements in the degree of global synchronization r are very hard to achieve, while improvements in the local synchronization r_{link} are easy to be generated by creating cliques of oscillators with similar native frequencies. For large C the system is locally already synchronized, thus the evolution of the network is guided by improvements towards a larger degree of global synchronization. In the case of intermediate C a trade-off between the above extremes is realized.

Figure 4 displays some prototypical results from optimization procedure for a choice of $\lambda = 1/2$. The total coupling $C = \sigma^* L$ is tuned by changing the interaction strength σ^*, while the number of links in the network is held constant. Panel (a) depicts an example network evolved for small σ^*. One notes the high cliquishness marked by groupings of oscillators with similar native frequencies.

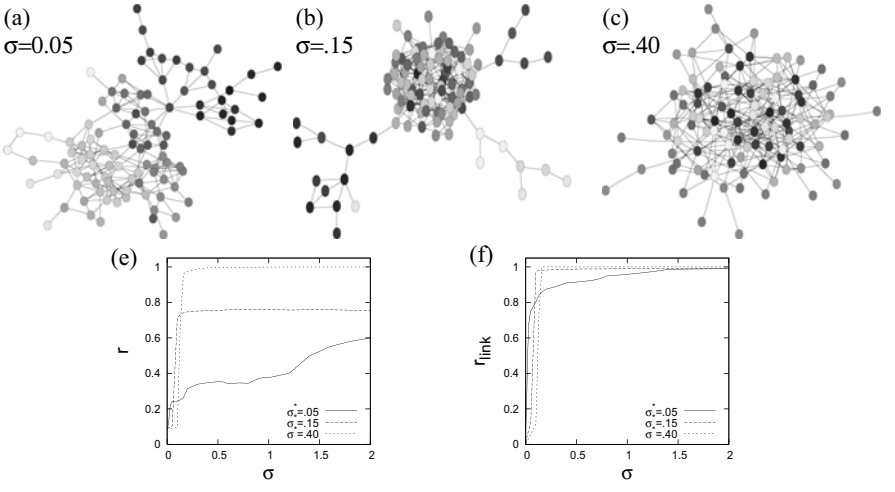

Fig. 4. Example networks with optimal synchronizability R constructed for (a) low coupling strength (b) intermediate coupling strength and (c) large coupling strength for $\lambda = 1/2$ (equal share of local and global synchronizability in R). Parameters are $N = 100, \langle k \rangle = 5$. The color of the nodes corresponds to the native frequency of the node, white nodes have $\omega = -1$ and black nodes $\omega = 1$ while different shades of gray interpolate between both situations. The lower panels (e) and (f) show the dependence of the global and local synchronizability on the coupling strength σ for the networks (a-c). Data points represent averages over 100 random initial conditions of the phases. Figure from [15].

The arrangement of the groups is a linear gradient, groups with oscillators of far-off the mean native frequencies $\omega = \pm 1$ being at both ends. The structure of this network is reflected in the synchronization transition, i.e. in the $r(\sigma)$ and the $r_{\text{link}}(\sigma)$ dependencies. Whereas $r_{\text{link}}(\sigma)$ rises steeply for small σ (corresponding to the formation of synchronized modules), the global synchronization order parameter r rises only gradually, showing distinct steps that are related to the merger (i.e. synchronization) of separate modules. However, the relatively loose coupling between modules and the strong intra-modular coupling make global synchronization very hard to attain.

In contrast, the panel Fig. 4c depicts a network which was evolved for large coupling strength. Here, one notes one tightly interwoven network core, which contains most of the oscillators with large magnitudes of their native frequencies. These nodes are nodes with more than the average number of links. The arrangement of these oscillators is such that anti-correlated pairings are formed. The periphery of the network is made up by nodes close to the mean (i.e. synchronization-) frequency. For this type of network the $r(\sigma)$ and $r_{\text{link}}(\sigma)$-dependencies almost coincide, local and global synchronization are attained for the same coupling strength. Put in other words: synchronization is attained via the formation of many small intrinsically synchronized clusters.

Fig. 4b illustrates an interpolating case, i.e. a system configuration evolved for intermediate coupling strength. The network is characterized by one tighly interwoven core which contains nodes of large native frequency magnitudes. As for case (c) these nodes are hub nodes. The periphery of the networks consists of tree-like cliques of oscillators with similar native frequencies that are only very loosely connected to the core. Here, the $r(\sigma)$ and $r_{\mathrm{link}}(\sigma)$ dependencies show a rapid onset of macroscopic synchronization, which can be attributed to the oscillators in the core. However, because only loosely connected to the core and being sustained by oscillators of similar native frequency in the periphery, periphery nodes are very hard to recruit into the synchronized cluster. Unless the coupling strength σ is very large, these nodes exhibit a dynamics that is largely independent of the synchronized dynamics of the core nodes.

3 Summary, Conclusions and Outlook

In this summary paper we have briefly outlined properties of systems of non-identical Kuramoto oscillators with enhanced synchronizabilities. As our most important point we stress that the structure of such systems is characterized by a correlated assignment of oscillators to nodes in such a way that oscillators with opposite signs of their respective native frequencies are paired. It is shown that oscillator correlations also systematically influence properties of the synchronization transition on complex networks. Positively and negatively correlated assignments are found to represent different regimes; properties of the synchronization transition are fundamentally different for both cases.

The results that we present in this paper are specific for the Kuramoto system. However, it appears that the findings indicate a general principle: optimal configurations are such, for which the time-averaged interaction term is maximized. First tentative results indicate that similar findings about the arrangement of the identities of oscillators on a network apply also for chaotic limit cycle oscillators.

In the last section of the paper we discuss that the requirements for local and global synchronization are conflicting demands on the system's organization. While the first is connected to cliquish arrangements with positive oscillator correlations, the second demands good mixing, i.e. anti-correlated arrangements and unclustered network topologies. This allows to conclude that systems, whose constituents aim for an optimization of their local synchronization with their neighbourhoods, cannot achieve global synchronization.

References

1. Winfree, A.T.: The Geometry of Biological Time. Springer, New York (1984)
2. Kuramoto, Y.: Chemical Oscillations, Waves, and Turbulence. Springer, Berlin (1984)
3. Manrubia, S.C., Mikhailov, A.S., Zanette, D.H.: Emergence of Dynamical Order. In: Synchronization Phenomena in Complex Systems. World Scientific, Singapore (2004)

4. Pluchino, A., Latora, V., Rapisarda, A.: Eur. Phys. J. B 50, 169 (2006)
5. Hill, D., Chen, G.: Power Systems as Dynamical Networks. Circuits and Systems, 722–725 (2006)
6. Arenas, A., Díaz-Guilera, A., Kurths, J., Moreno, Y., Zhou, C.: Synchronization in Complex Networks. Phys. Rep. (in press) (2008)
7. Albert, R., Barabási, A.-L.: Rev. Mod. Phys. 47, 47 (2002)
8. Newman, M.E.J.: SIAM Rev. 45, 167 (2003)
9. Pecora, L.M., Carroll, T.M.: Master Stability Functions for Synchronized Coupled Systems. Phys. Rev. Lett. 80, 2109–2111 (1998)
10. Donetti, L., Hurtado, P.I., Muñoz: Phys. Rev. Lett. 95, 188701 (2005)
11. Boccaletti, S., Latora, V., Moreno, Y., Chavez, M., Hwang, D.-U.: Complex Networks: Structure and Dynamics. Phys. Rep. 424, 175–308 (2006)
12. Acebrón, J.A., Bonilla, L.L., Pérez Vicente, C.J., Ritort, F., Spigler, R.: The Kuramoto Model: A simple Paradigm for Synchronization Phenomena. Rev. Mod. Phys. 77, 137–185 (2005)
13. Brede, M.: Synchrony-optimized Networks of Non-Identical Kuramoto Oscillators. Phys. Lett. A 372, 2618–2622 (2008)
14. Brede, M.: Construction Principles for Highly Synchronizable Sparse Directed Networks. Phys. Lett. A 372, 5305–5308 (2008)
15. Brede, M.: Local vs. Global Synchronization in Networks of Non-Identical Kuramoto Oscillators. Eur. Phys. J. B 62, 87–94 (2008)
16. Brede, M.: The Synchronization Transition in Correlated Oscillator Populations (preprint, 2008), arXiv:0810.1121v1
17. Brede, M.: Synchronization on Directed Small Worlds: Feed Forward Loops and Cycles. Europhys. Lett. (to appear) (2008) (preprint), arXiv:0809.2117v1
18. Son, S.-W., Jeong, H., Hong, H.: Relaxation of Synchronization on Complex Networks. Phys. Rev. E 78, 016106 (2008)
19. Hong, H., Choi, M.Y., Kim, B.J.: Synchronization on Small-World Networks. Phys. Rev. E 65, 026139 (2002)
20. Moreno, Y., Pacheco, A.F.: Synchronization of Kuramoto Oscillators in Scale-Free Networks. Eurphys. Lett. 68, 603–609 (2004)
21. Gómez-Gardeñes, J., Moreno, Y.: Synchronization of Networks with Variable Local Properties. Int. J. Bif. and Chaos 17, 2501 (2007)
22. Lee, D.-S.: Synchronization Transition in Scale-Free Networks: Clusters of Synchrony. Phys. Rev. E 72, 026208 (2005)
23. Gómez-Gardeñes, J., Moreno, Y., Arenas, A.: Paths to Synchronization on Complex Networks. Phys. Rev. Lett. 98, 034101 (2007)
24. Gómez-Gardeñes, J., Moreno, Y., Arenas, A.: Synchronizability Determined by Coupling Strengths and Topology on Complex Networks. Phys. Rev. E 75, 066106 (2007)